ORIGINAL RESEARCH

Laryngoscope
Investigative Otolaryngology

Jet flow rate and needle position govern distal airway pressures during low-frequency jet ventilation

Joshua Pertile MS[1] | Bradford Smith PhD[1,2] | Michelle Mellenthin PhD[1,3] | Jennifer Wagner B.S., R.T. (R)[1] | Emily M. DeBoer MD, MSCS[2] | Daniel S. Fink MD[4]

[1]Department of Bioengineering, University of Colorado Denver, Anschutz Medical Campus, Aurora, Colorado, USA

[2]Department of Pediatrics, School of Medicine, University of Colorado, Aurora, Colorado, USA

[3]Department of Computer Science and Engineering, Colorado Mesa University, Grand Junction, Colorado, USA

[4]Department of Otolaryngology, School of Medicine, University of Colorado, Aurora, Colorado, USA

Correspondence
Daniel S. Fink, MD, Department of Otolaryngology, School of Medicine, University of Colorado, 12631 E. 17th Ave, B-205, Aurora, CO 80045.
Email: daniel.fink@cuanschutz.edu

Funding information
The American Laryngological Association Voice and Research Education Grant

Abstract

Objectives: Although jet ventilation is frequently used during surgery for airway stenosis, little is known about distal airway pressures during jet ventilation. The objective of the study is to determine how jet pressure, flow rate, and position of the ventilation needle relate to distal airway pressure magnitude and homogeneity.

Methods: Two 3D models of the first five generations of the human airway tree were created. One is a duplicate of a human airway from a 15-year-old healthy male's computed tomography scan, and the other is an idealized symmetric model of human lung morphometry. Pressure transducers measured fifth-generation distal airway pressures in both models. A computer-controlled jet needle positioning system was used to ventilate the lung casts. The effects of jet needle position, jet pressure, and jet flow rate on distal airway pressure and homogeneity were measured.

Results: Total entrained jet flow rate was the most reliable predictor of distal airway pressure. Pressure supplied to the jet ventilation needle had a positive linear relationship with distal airway pressure; however, this relationship was dependent on the jet needle flow resistance. As the ventilation needle moved closer to the tracheal wall, ventilation homogeneity decreased. Depth into the trachea was positively correlated with sensitivity of the needle to the tracheal wall.

Conclusion: In this model, total entrained jet flow rate is a more robust predictor of distal airway pressure than jet inlet pressure. More homogeneous ventilation was observed in our model with the ventilation needle centered in the proximal region of the trachea.

KEYWORDS
flow, homogeneity, jet ventilation, pressure

INTRODUCTION

Low-frequency jet ventilation (LFJV) is a widely used form of ventilation. It is frequently employed during direct laryngoscopy or rigid bronchoscopy, when intubation is not possible or would obscure the surgical field, as well as in emergency ventilation scenarios.[1-3] Ventilation is provided in bursts through a needle at relatively high pressures, and the jet needle is typically mounted in a scope, such as a laryngoscope, with expiration being passive. Jet ventilation is performed in an open system, unlike standard ventilation through a cuffed

endotracheal tube, making the measurement of distal airway pressures quite challenging. In LFJV, an anesthesia provider generally manually controls the delivery of jet pressure between 10 and 24 breaths per minute. This is in contrast to high-frequency jet ventilation, in which an automated ventilator generally delivers 60 to 150 breaths per minute. There are a wide range of methods utilized by airway teams to prescribe LFJV pressures or flow rates.[4-6] This may be because the equations correlating distal airway pressures (P_{distal}) with jet pressure (P_{jet}) or flow rate have not yet been established, leaving airway teams to rely on personal experience and training rather than evidence-based guidelines. As such, methods to set pressure vary by provider and institution. Many airway teams set pressure by feeling for the correct P_{jet} on their forearm whereas others start at a low pressure and then slowly increase pressure during ventilation until the visual chest rise is deemed adequate.[5,6]

The needle mounting position is also not standardized between different scope models. Depending on the model the depth and position of the needle will vary. This is an important consideration since changes in endotracheal tube angle in intubated patients can significantly change regional ventilation distribution.[7] Accordingly, we hypothesize that different needle placements and depths may cause changes in distal airway pressure and homogeneity.

To better understand the relationship between P_{jet} and P_{distal}, and to better understand the effect of jet needle placement within the airway, we developed a benchtop experimental system to simulate the dynamics of LFJV. Using this setup, we measured the effect of needle position and depth in the trachea on distal airway pressure homogeneity. In addition, we quantified the relationships between pressure supplied to the ventilation needle, total entrained flow from the jet needle, and distal airway pressure.

MATERIALS AND METHODS

Two physical models of the human airway tree were created. The first model is the *idealized model* that includes the first five airway generations and is symmetric in the sagittal and coronal planes (Figure 1A). The design is unique to this experiment with the branch angle, size, and airway caliber derived from the literature.[8-11] The first generation is a 125-mm long, 18-mm diameter trachea. Each of the four subsequent bifurcations has a 70° branch angle, and the plane of each bifurcation is rotated perpendicular to the previous bifurcation about the axis of the superior duct and the diameter at each daughter generation was 79% of the size of diameter of the superior airway. Each generation, except for the trachea, maintained a diameter to length ratio of 1:3.

The second model is a full-size fabrication based on an X-ray computed tomography (CT) scan from a healthy 15-year-old human male subject as previously described,[12] shown in Figure 1B. This geometry is referred to as the *CT model*. In both models, a positive cast of the airway tree was 3D printed at 100% size and encased in silicone. The print was dissolved away leaving a solid silicone block with hollow airways. Pressure transducers (Honeywell HSCDANN001PGAA5, Charlotte, North Carolina) were inserted at the end of the fifth-generation airways in
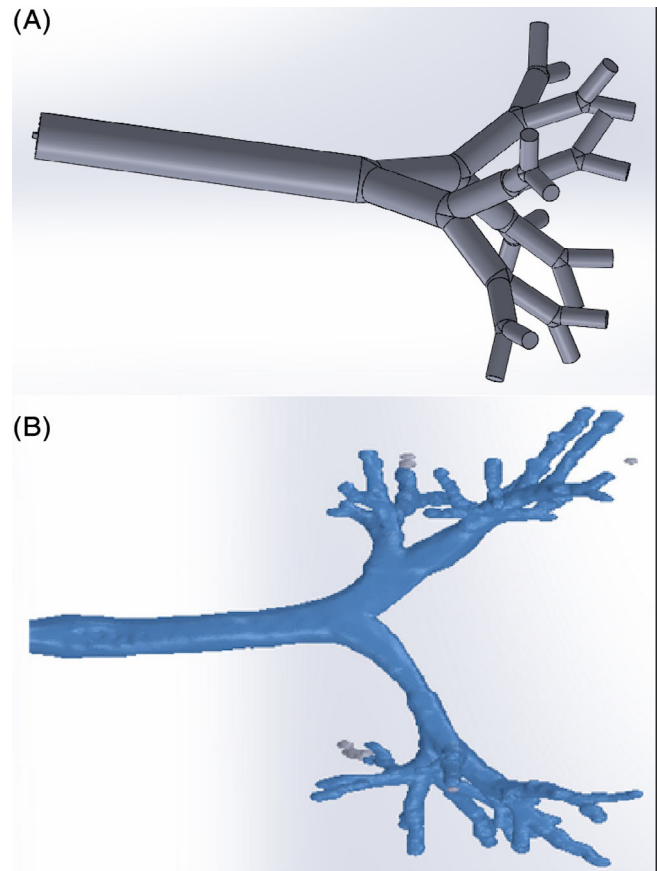

(A)

(B)

FIGURE 1 A, This shows the idealized airway geometry based on the Weibel geometry. B, This shows a model of the human airway tree derived from the computed tomography scan of a 15-year-old healthy human subject

each lobe of the lung in the CT model, and each of the 16 distal airways (fifth generation) for the idealized model. The transducers were inserted by drilling 3/8-inch holes in the cured silicone, affixing barbed fittings to the model with silicone adhesive, and coupling the transducer to the fitting with a short piece of flexible silicone tubing (Figure 2). The ends of the airways were sealed so that our measurements represent the end of a prolonged inspiration in clinical practice, where there is no net flow into or out of the lung. The duration of the experimental jet pulse was 3 seconds, and each measurement was separated by a minimum period of 1.75 seconds with no flow from the jet.

An automated system was constructed to control the position of the jet ventilation needle. A 3D printer with a precision of 200 μm (Anet A8, Shenzhen, China) was used as the base of the system, and a fixture was designed to hold the lung cast in place on the printing platform. Another fixture was designed to hold a 100-mm 14-gauge Luer Lock ventilation needle (Dispense All DA-4I-BDT, Chicago, Illinois) where the printer extrusion head was originally located. The gas delivery system (Figure 3) was comprised of an air compressor (California Air Tools 2050A, San Diego, California) connected to a pressure regulator and air dryer (PneumaticPlus SAW-2000M-N02BG, Torrance, California) and then a 10-gallon expansion chamber (California Air Tools AUX10, San Diego, California) that was included to provide a stable pressure source. Next,
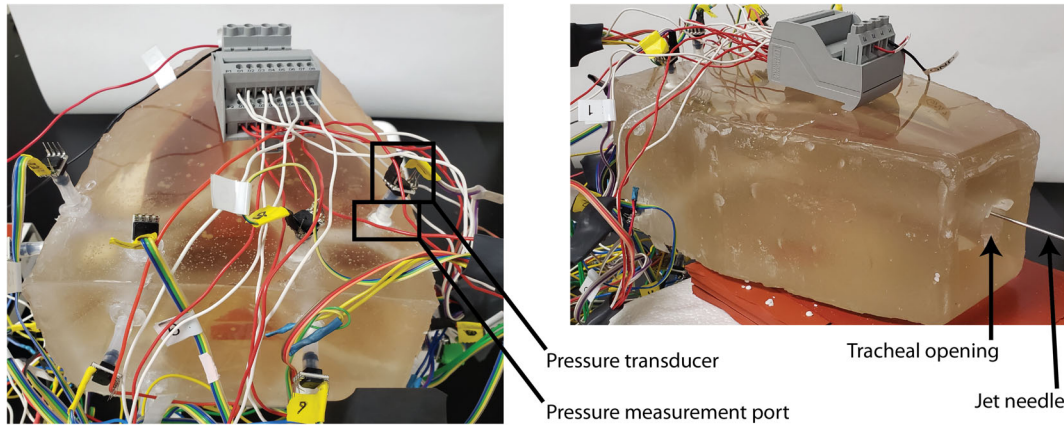
FIGURE 2   Photograph of the idealized model showing the pressure transducers, pressure measurement ports, tracheal opening, and jet needle
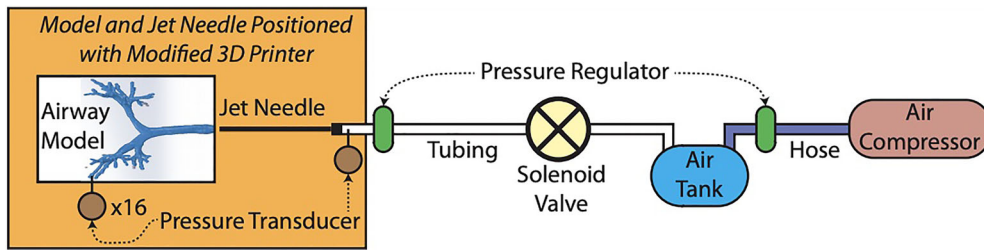

FIGURE 3   Schematic of the experimental configuration. Gas from an air compressor (red) travels through 3/8″ rubber hose (purple) and a pressure regulator (green) before entering an accumulator tank (blue). Compressed air leaves the tank through 1/4″ tubing (white) and passes through an electronically controlled solenoid valve (yellow) and a second pressure regulator. A pressure transducer (brown) is located immediately adjacent to the jet needle (black). The position of the jet needle in the lung model is controlled by a modified 3D printer. Sixteen pressure transducers report the distal airway pressures in the model

the gas passed through an electric solenoid valve (ASCO Red Hat 8262H002, Novi, Michigan) to allow for automatic, electrically actuated ventilation. The valve was controlled by the modified 3D printer to synchronize jet needle movement and gas delivery. A second pressure regulator (Norgren R46-200-RNLA, Littleton, Colorado) was positioned adjacent to the jet needle and a pressure transducer (Honeywell HSCDANN060PGAA5, Charlotte, North Carolina) that measured P_{jet}. Because P_{jet} is measured through a port that is flush with the tubing wall those pressures are termed a "static pressure," despite measuring a moving fluid, because the pressures do not include contributions from inertial forces. A separate device based on a venturi flow meter was created to measure total entrained flow rate (Q_{jet}) from the ventilation needle.

The automated test apparatus ventilated the model airway trees in 13 different positions in the tracheal cross-section (Figure 4). This was repeated for seven depths into the trachea. We define the jet needle depth as the distance of the needle past the entrance of the airway model, the level of the larynx. Placements for the CT model and idealized model started with the needle 1 cm into the trachea at 11.5 and 11.9 cm from the carina respectively and each placement was 1 cm deeper than the previous. Since the two tracheas had different shapes and diameters, we elected to maintain a consistent final distance of the needle and spacing of each step from the tracheal wall
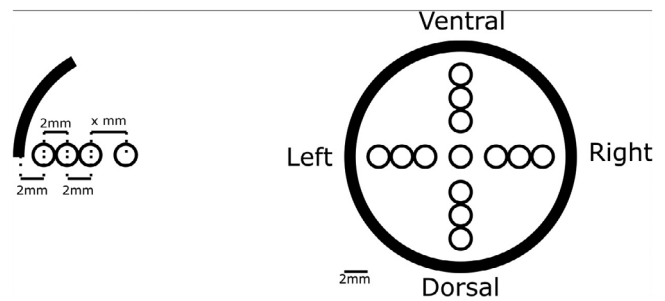

FIGURE 4   The left side shows the spacing dimensions of the needle positions relative to the tracheal wall. The right side shows a top-down view of the trachea with the 13 ventilation needle positions including the center and three steps in each direction. This pattern of 13 positions was repeated a seven needle depths into the trachea

across models. In the positions closest to the edges of the trachea, the center of the needle was 2 mm from the wall of the trachea. This provided a gap of just under 1 mm between the tracheal wall and the outside wall of the needle. The next two needle positions were on a 2-mm spacing and the final step, which placed the needle in the center of the trachea, varied with the model geometry (Figure 4).

RESULTS

The relationship between P_{jet} and P_{distal} was established in the idealized and CT models seen in Figure 5. We have based our analysis on the jet inlet pressure (P_{jet}) because this parameter is frequently available via an analog pressure gauge during clinical application of manual jet ventilation. In both cases, a piecewise linear fit was used to account for the more rapid increase in P_{Distal} with P_{Jet} that occurs at higher P_{Jet}. The breakpoint in the piecewise linear fits occurred at approximately 250 cm H_2O for the idealized model (Figure 5A) and 700 cm H_2O for the CT model (Figure 5B). Since these pressures are far below clinical P_{Jet}, we report and show only the upper segment of the linear fit in Equation (1) (CT model) and Equation (2) (idealized model).

$$P_{distal} = 0.0064 * P_{jet} - 3.1, \tag{1}$$

$$P_{distal} = 0.0065 * P_{jet} - 1.25. \tag{2}$$

The total entrained jet flow rate (Q_{jet}) includes the flow rate moving through the needle, and the ambient air entrained into the jet flow. In the idealized model, the relationship exhibited between P_{distal} and Q_{jet} can be approximated with a simple quadratic equation (Equation (3)) shown in Figure 6A.

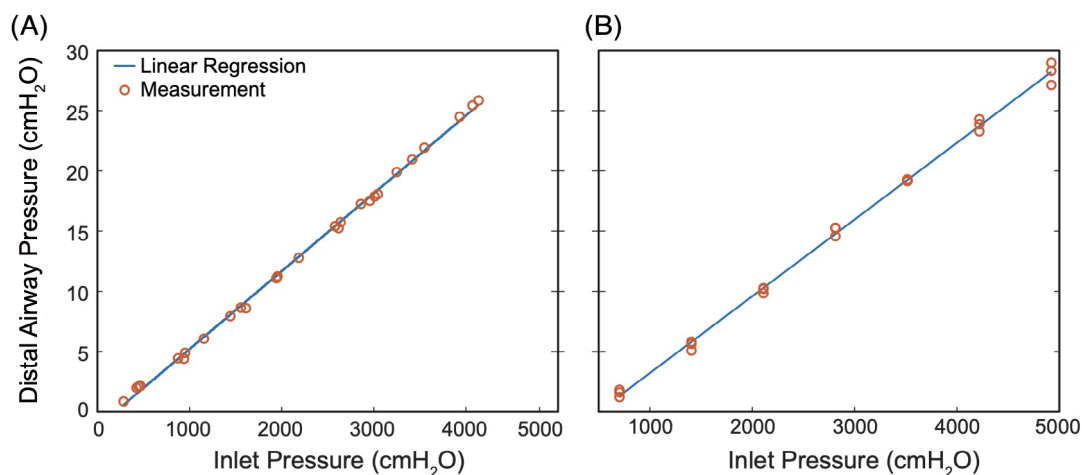$$P_{distal} = 3.43 * Q_{jet}^2 - 0.64 * Q_{jet} + 0.18. \tag{3}$$

FIGURE 5 A, Linear regression (line) and measured data (points) of P_{jet} vs P_{distal} for the idealized model with the needle centered and 1 cm into the trachea (11.5 cm from the carina). B, Linear regression (line) and measured data (points) of inlet pressure (P_{jet}) vs distal airway pressure (P_{distal}) for the computed tomography model with the needle centered and 1 cm into the trachea (11.9 cm from the carina). For each pane, a piecewise linear fit was established and only the upper portion of the piecewise fit is shown
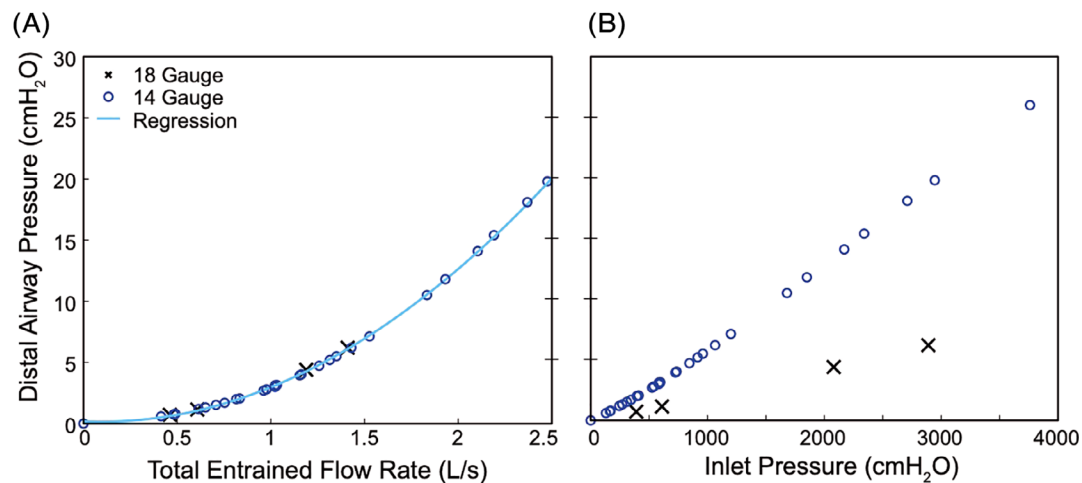

FIGURE 6 A, The relationship between total entrained jet flow and distal airway pressure in the idealized block. B, The relationship between jet inlet pressure and distal airway pressure with the jet needled centered 1 cm into the trachea (11.9 cm from the carina) in the idealized block. For both panes, blue circles indicate a 14-gauge jet needle and black × symbols indicate an 18-gauge jet needle
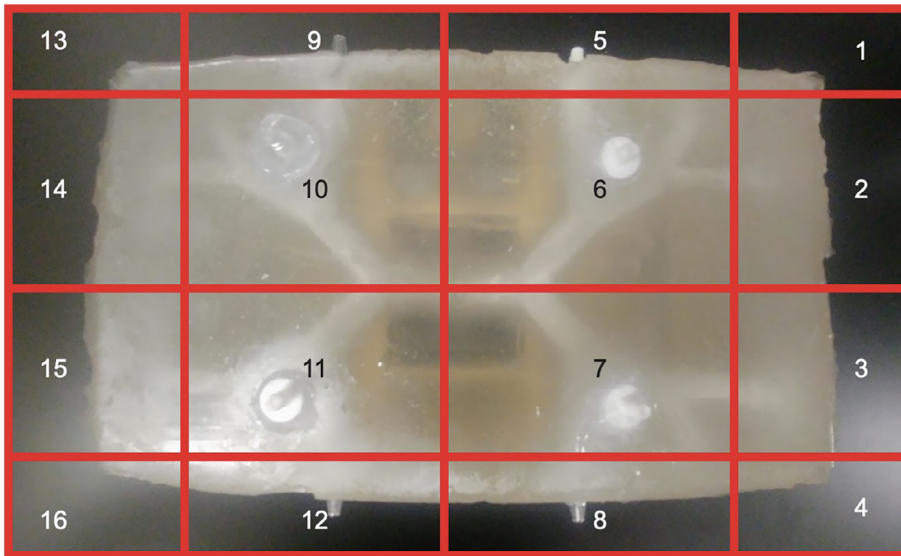
FIGURE 7 The numbered positions of the sensors on the idealized model looking upwards from the base of the lung. The top and the bottom of the image represent the anterior and posterior of the lungs respectively, and are shown in the same manner on the homogeneity grids. The left side of the image represents the right lung, shown on the left side in the homogeneity grids. Pressure transducer location numbers correspond to the homogeneity grid show in Figure 8
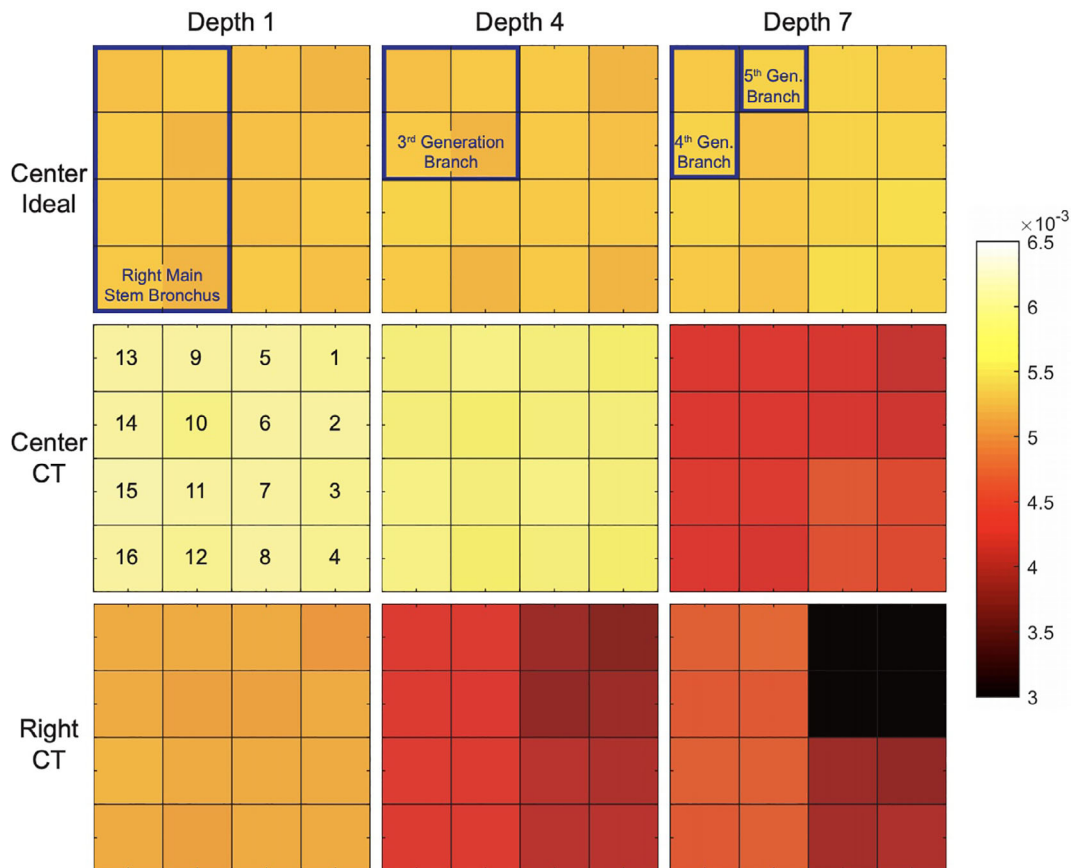

FIGURE 8 This figure is a comparison of homogeneity in the distal airways at 1, 4, and 7 cm deep into the trachea. Row 1 shows the idealized model with the needle centered in the trachea. Row 2 shows the CT model with the needle entered in the trachea. Row 3 shows the computed tomography (CT) model with the needle at the third step to the right, which is 2 mm from the right wall of the trachea. In the idealized model and the CT model the trachea was 12.5 and 12.9 cm long, respectively. The distance from the carina is the tracheal length minus the depth into the trachea. Numbers correspond to the pressure sensor locations in Figure 7. The jet pressure is 1500 cm H_2O which corresponds to a jet flow rate of ≈1.65 L/s

The relationship between Q_{jet} and distal airway pressure is consistent across different needle gauges. Figure 6B (circles) shows the continuous piecewise linear relationship between inlet pressure and distal airway pressure.

The black 'x' symbols in Figure 6 show ventilation with an 18-gauge needle. With the same P_{jet}, changing the needle from 14 to 18 gauge reduces Q_{jet} and causes decreased distal airway pressure in

accordance with the relationship shown in Figure 6A (Equation (3)). While using a consistent ventilation setup (including needle diameter and length), any given P_{jet} correlates to a single Q_{jet}. Using live readings from the flowmeter and P_{jet} data, we calculated the conversion factor from P_{jet} to Q_{jet}. With this equation the piecewise linear relationship in Figure 6B can converted to Figure 6A. Because clinical jet ventilation is guided by P_{jet} we have performed the remainder of the analysis using that parameter. The reported pressures shown are normalized to P_{jet} so that the normalized pressure $P_{norm} = P_{distal}/P_{jet}$ (Equation (4)). This removes variation due to temporal fluctuations in P_{jet} and provides the data in a dimensionless form.

To analyze the spatial distribution of airway pressure in the fifth airway generation, we have created plots that we refer to as *homogeneity grids*. These grids graphically depict the pressures in the fifth-generation airways, with each tile representing the pressure in a single airway. In the case of perfectly homogenous ventilation, the color will be uniform across the homogeneity grid. In the case of heterogeneous ventilation, the fifth-generation airway pressures will not be uniform and the grid tiles will have different colors. The spatial layout of these grids is shown superimposed on the idealized model in Figure 7. The first row of Figure 8 shows homogeneity grids for the needle centered

at depths 1, 4, and 7 cm for the idealized model. Row 2 of Figure 8 shows the same ventilation applied to the CT model. In both cases, the jet pressure is 1500 cm H_2O which corresponds to a jet flow rate of ≈1.65 L/s. The same ventilation points on the CT model resulted in much larger changes in P_{distal} and pressure homogeneity. The model did not show a substantial change in pressure with respect to depth of needle placement. At a depth of 7 cm in the CT model (5.5 cm from the carina), even a millimeter of movement toward one of the tracheal walls could result in heterogeneous ventilation.

Note that with a needle placement in the right side of the trachea (Figure 8, third row), the left lung saw increased ventilation. This only occurred with the needle pointing straight into the trachea. A centered needle that was angled toward one side would hyperventilate the ipsilateral lung as seen in other literature.[7] If the tip of the needle was held to one side of the trachea and the needle angle was manually adjusted in the coronal plane, there was an abrupt discontinuity as the angle approached 0° where the contralateral lung was suddenly hyperventilated.

The data from the heterogeneity grids are summarized in Figure 9 which shows the range of pressures in the idealized and CT models at varied distances and directions from the center of the trachea. In

FIGURE 9 All panels of this figure shows the homogeneity in distal airway pressure in the idealized and computed tomography (CT) model as a function of jet needle depth past the laryngeal folds and lateral placement. The dark line in the center for each position shows the combined mean of all the distal airway sensors for the 3 seconds of ventilation at that depth. The shaded area represents the range from the highest to lowest mean value for any individual sensor at that needle depth. The steps toward the wall are numbered from the center of the trachea out. Left 1 is closest to the center and left 3 is closest to the left side of the tracheal wall. The lateral placements shown in the second column are in the designated direction closest to the tracheal wall. In the idealized model and the CT model the trachea was 12.5 and 12.9 cm long, respectively, so the distance from the carina is the tracheal length minus the depth into the trachea. The jet pressure is 1500 cm H_2O which corresponds to a jet flow rate of ≈1.65 L/s
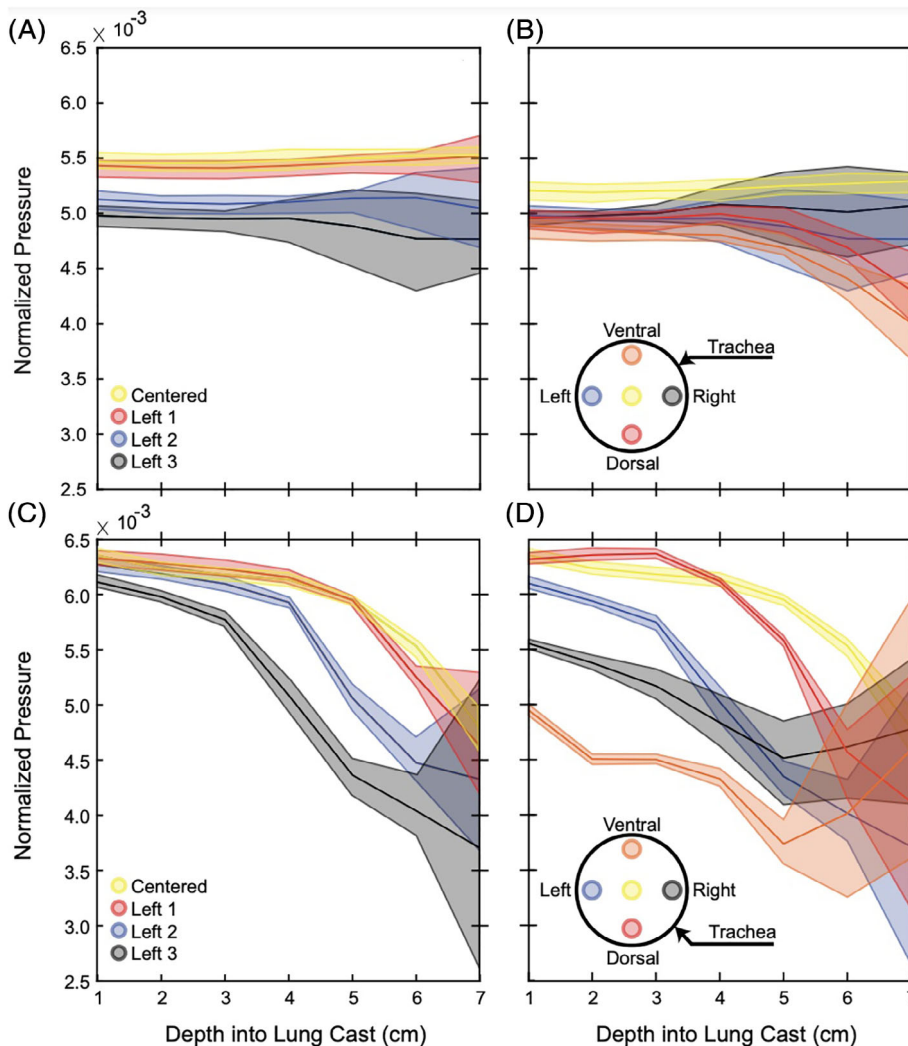
nearly every case in both airway models, the ventilation pressure in the distal airways became more heterogeneous as the ventilation needle was moved distal or laterally in the trachea. The sensitivity to lateral placement increased with depth into the trachea.

Figure 9B,D shows the homogeneity graphs comparing the center placement and the most lateral placement each direction. For all directions, the pressure was relatively homogeneous for proximal needle positions and the normalized pressures were approximately equal. At more distal needle positions homogeneity decreased and the homogeneity of distal airway pressure became more sensitive to small changes in needle placement. The sensitivity of the system to needle position was more pronounced in the CT model than in the idealized model.

DISCUSSION

Although LFJV has been shown to be safe overall, it is generally only used in specialized centers and is often either avoided or suboptimally employed due to a limited understanding optimal ventilation practices. Avoidance of jet ventilation may lead to unnecessary intubations. Insufficient pressures during LFJV may lead to insufficient end-expiratory pressures causing cyclic airspace collapse and reopening (atelectrauma) while applying excessive pressure can result in over-distension (volutrauma).[13,14] Heterogeneous ventilation reduces the overall quality of ventilation and increases the risk of ventilator-induced lung injury, which is an acute injury caused by volutrauma and atelectrauma.[13] Accurate estimations of P_{distal} and methods for increasing ventilation homogeneity are essential tools in reducing the primary causes of complications during ventilation including excessive pressure, insufficient inspiratory pressures, and insufficient positive end-expiratory pressure.

In our experimental model, central needle placement within the trachea and placement more proximally within the trachea were both effective at promoting ventilation homogeneity. Jet ventilation was consistently able to provide homogeneous ventilation with proximal placements independent of lateral position. With more distal needle placements, the distribution of airway pressures was more sensitive to lateral placements. In the CT model, at 1 cm past the entrance to the airway, homogenous ventilation was demonstrated at all lateral positions, whereas at depth of 7 cm, a few millimeters of difference from the center created marked pressure heterogeneity (Figures 8 and 9). We hypothesize that the trachea, acting as a tube entrance length, will produce a fully developed flow regime given enough length to do so, and a longer entrance length will more effectively develop the flow.

In our model, pressure at the needle (P_{jet}) was only predictive of P_{distal} if the same ventilation equipment (eg, jet needle) and needle position was used each time. The total entrained jet flow rate (Q_{jet}), which includes the flow rate moving through the needle, and the ambient air entrained into the jet flow, combined with needle placement parameters was more predictive of distal airway pressure. Further experimentation with more refined models will be beneficial in confirming the relationship between Q_{jet}, needle placement and distal

airway pressure across different needle gauges and setup configurations.

There are limitations with these benchtop models of jet ventilation. The absence of distensible parenchyma in our model means that there is no volume change with applied airway pressure as would be noted in vivo. Since the silicone material used to create the airway trees is quite firm (50 durometer), the trachea will not deform due to jet pressure as would occur with tissue. Finally, our model terminates at the fifth generation, although enough airway appears to be included to capture heterogeneity between different lung lobes.[15]

CONCLUSION

We have developed a system to reliably position a LFJV needle in idealized and patient-specific airway models. Our experimental analysis shows that physiologically preferred homogeneous ventilation is best achieved with the jet needle positioned proximally and centrally in the trachea. As the depth of the jet needle in the trachea is increased, the sensitivity of the system to the radial position of the jet needle in the trachea is increased. Finally, in this model, the entrained flow rate from the jet needle provides the most robust correlation with distal airway pressures. Further experimentation with different pressures and more physiologic models would be beneficial in confirming optimal surgical practices.

CONFLICT OF INTEREST
The device to measure total entrained flow rate has been patented by the authors (62/857,197).

ORCID
Joshua Pertile https://orcid.org/0000-0002-9343-4873
Bradford Smith https://orcid.org/0000-0002-1583-6762
Daniel S. Fink https://orcid.org/0000-0001-5162-2537

REFERENCES
1. Baraka AS, Siddik SS, Taha SK, Jalbout MI, Massouh FM. Low frequency jet ventilation for stent insertion in a patient with tracheal stenosis. *Can J Anesth* 2001;48(7):701–704.
2. Pathak V, Welsby I, Mahmood K, Wahidi M, MacIntyre N, Shofer S. Ventilation and anesthetic approaches for rigid bronchoscopy. *Ann Am Thorac Soc* 2014;11(4):628–634.
3. Duggan LV, Ballantyne Scott B, Law JA, Morris IR, Murphy MF, Griesdale DE. Transtracheal jet ventilation in the "can't intubate can't oxygenate" emergency: a systematic review. *Br J Anaesth* 2016;117 (Suppl 1):i28–i38.
4. Rames Philips BS, DeSilva B, Matrka L. Jet ventilation in obese patients undergoing airway surgery for subglottic and tracheal stenosis. *Laryngoscope* 2017;128(8):1887–1892.
5. Barry RA, Fink DS, Pourciau DC, et al. Effect of increased body mass index on complication rates during laryngotracheal surgery

utilizing jet ventilation. *Otolaryngol Head Neck Surg* 2017;157(3): 473–477.

6. University of Iowa Healthcare. Jet ventilation anesthesia—transoral for laryngeal surgery. *Iowa Head and Neck Protocols* 2019; https:// medicine.uiowa.edu/iowaprotocols/jet-ventilation-anesthesia-transoral-laryngeal-surgery. Accessed June 18, 2019.

7. Lumb AB, Burns AD, Figueroa Rosette JA, Gradzik KB, Ingham DB, Pourkashanian M. Computational fluid dynamic modelling of the effect of ventilation mode and tracheal tube position on air flow in the large airways. *Anaesthesia* 2015;70(5):577–584.

8. Florens M, Sapoval B, Filoche M. An anatomical and functional model of the human tracheobronchial tree. *J Appl Physiol* 2011;110(3):756–763.

9. Horsfield K, Dart G, Olson DE, Filley GF, Cumming G. Models of the human bronchial tree. *J Appl Physiol* 1971;31(2):207–217.

10. Weibel ER. *Morphometry of the Human Lung*: Heidelberg, Germany: Academic Press; 1963.

11. Michiels C. Physiological and pathological responses to hypoxia. *Am J Pathol* 2004;164(6):1875–1882.

12. DeBoer EM, Wagner J, Kroehl ME, et al. Three-dimensional printed pediatric airway model improves novice learners' flexible bronchoscopy skills with minimal direct teaching from faculty. *Simul healthc J Soc Simul Healthc* 2018;13(4):284–288.

13. Bilek AM, Dee KC, Gaver DP III. Mechanisms of surface-tension-induced epithelial cell damage in a model of pulmonary airway reopening. *J Appl Physiol* 2003;94:770–783.

14. Kay SS, Bilek AM, Dee KC, Gaver DP III. Pressure gradient, not exposure duration, determines the extent of epithelial cell damage in a model of pulmonary airway reopening. *J Appl Physiol* 2004;97:269–276.

15. Smith BJ. Strain heterogeneity in the injured lung: cause or consequence? *J Appl Physiol* 2016;121(6):1363–1364.